



PERGAMON

Journal of the Mechanics and Physics of Solids
48 (2000) 1541–1563

JOURNAL OF THE
MECHANICS AND
PHYSICS OF SOLIDS

www.elsevier.com/locate/jmps

A micromechanically-based constitutive model for frictional deformation of granular materials

Sia Nemat-Nasser

*Center of Excellence for Advanced Materials, Department of Mechanical and Aerospace Engineering,
University of California, San Diego, La Jolla, CA 92093-0416, USA*

Received 26 April 1999; received in revised form 17 October 1999

Abstract

A micromechanically-based constitutive model is developed for inelastic deformation of frictional granular assemblies. It is assumed that the deformation is produced by relative sliding and rolling of granules, accounting for pressure sensitivity, friction, dilatancy (densification), and, most importantly, the fabric (anisotropy) and its evolution in the course of deformation. Attention is focused on two-dimensional rate-independent cases. The presented theory fully integrates the micromechanics of frictional granular assemblies at the micro- (grains), meso- (large collections of grains associated with sliding planes), and macro- (continuum) scales. The basic hypothesis is that the deformation of frictional granular masses occurs through simple shearing accompanied by dilatation or densification (meso-scale), depending on the microstructure (micro-scale) and the loading conditions (continuum-scale). The microstructure and its evolution are defined in terms of the fabric and its evolution. While the elastic deformation of most frictional granular assemblies is rather small relative to their inelastic deformation, it is included in the theory, since it affects the overall stresses. © 2000 Elsevier Science Ltd. All rights reserved.

Keywords: Granular materials; Micromechanical models; Friction

1. Introduction

A physically-based constitutive model is developed by Balendran and Nemat-

E-mail address: ceam@ames.ucsd.edu (S. Nemat-Nasser).

0022-5096/00/\$ - see front matter © 2000 Elsevier Science Ltd. All rights reserved.
PII: S0022-5096(99)00089-7

Nasser (1993a, 1993b) by considering the frictional anisotropic deformation of cylindrical granular masses and Coulomb's friction criterion. This model predicts rather well the observed dilatancy and densification effects in monotonic and cyclic loading. The model is based on the *double-sliding* mechanism originally proposed by Mandel (1947), and further developed by de Josselin de Jong (1959), Spencer (1964, 1982) and Mehrabadi and Cowin (1978).

The present work seeks to integrate the experimentally observed response of two-dimensional frictional granules into a general theory which includes the above-cited theories as special cases; a comprehensive account of these and related results is contained in an upcoming book by the author. Experiments on various assemblies of two-dimensional photoelastic rods of oval cross section, deformed under biaxial loads and in simple shearing, have shown that:¹

1. the distributions of the unit contact normals \mathbf{n} , and the unit branch vectors² \mathbf{m} , are essentially the same and may be used interchangeably;
2. the fabric tensors $\langle \mathbf{n} \otimes \mathbf{n} \rangle$ and $\langle \mathbf{m} \otimes \mathbf{m} \rangle$ are essentially the same, where $\langle \phi \rangle$ denotes the volume average of ϕ ;
3. the diagonal elements of these fabric tensors are almost constant in simple shearing under a constant confining pressure;
4. the off-diagonal elements of these fabric tensors behave similarly to the applied shear stress; and
5. the second-order distribution density function of the unit contact normals, $E(\mathbf{n})$, which is essentially the same as that of the unit branch vectors, $E(\mathbf{m})$, is represented by

$$E(\mathbf{n}) \frac{1}{2\pi} \{1 + \mathcal{E} \cos(2\theta - 2\theta_0)\}, \quad (1a)$$

where $\mathcal{E} = (\frac{1}{2} \mathcal{E}_{ij} \mathcal{E}_{ij})^{1/2}$ is the second invariant of the fabric tensor \mathcal{E} , of components (in two dimensions)

$$\mathcal{E}_{ij} = 4 \left(\mathcal{J}_{ij} - \frac{1}{2} \delta_{ij} \right), \quad (1b)$$

where $\mathcal{J}_{ij} = \langle n_i n_j \rangle$; \mathcal{E} defines the degree of anisotropy of distribution (Eq. (1a)), and θ_0 gives the orientation of the greatest density of the contact normals; $\theta_0 + \frac{\pi}{2}$ then gives the orientation of the least density; see Subhash et al. (1991) and Balendran and Nemat-Nasser (1993a).

¹ See Oda et al. (1982, 1985) and Subhash et al. (1991).

² A vector connecting the centroids of two contacting granules, is called a branch vector, and the corresponding unit vector is the unit branch vector.

2. Sliding resistance

It may be assumed that the overall deformation of a granular mass consists of a number of dilatant simple shearing deformations, along the active shearing planes. At the micro-scale, this dilatant simple shear flow occurs on active shearing planes through sliding and rolling of grains over each other at active contacts. In a granular sample with a large number of contacting granules, a mesoscopic shearing plane passes through a large number of contacting granules with various orientations of contact normals. Fig. 1(a) schematically shows the mesoscopic shearing plane with the unit normal vector \mathbf{v} , a typical set of contacting granules, and the shearing direction defined by the unit vector \mathbf{s} . For future referencing, this plane will also be called the *sliding plane*, even though both particle rolling and sliding are involved at the micro-scale.

The resistance to the dilatant simple shearing is provided by the average of the contact forces which are transmitted across the sliding plane. These forces depend on the local frictional properties of the contacting granules, as well as on their relative arrangement, i.e., the fabric of the granular mass. The tractions transmitted across a plane of unit normal \mathbf{v} , are given by

$$\bar{\mathbf{t}}^{(v)} = \mathbf{v} \cdot \left\{ 2N\bar{l} \int_{\Omega_{1/2}} E(\mathbf{n})\mathbf{n} \otimes \hat{\mathbf{f}} d\Omega \right\}, \quad (2a)$$

where the overall Cauchy stress is defined by (Christoffersen et al., 1981)

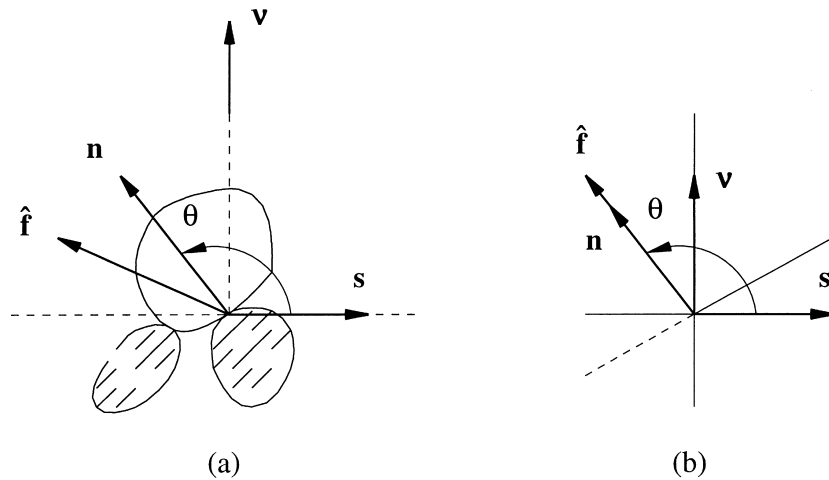


Fig. 1. Schematic representation of a mesoscopic dilatant shearing plane with unit normal \mathbf{v} : (a) a typical set of contacting granules, and the sliding direction defined by the unit vector \mathbf{s} ; and (b) a simple model for estimating the resistance to sliding, $\bar{\tau}_{\text{fab}}$, due to fabric.

$$\bar{\boldsymbol{\sigma}} = 2N\bar{l} \int_{\Omega_{1/2}} E(\mathbf{n})\mathbf{n} \otimes \hat{\mathbf{f}} \, d\Omega. \quad (2b)$$

Here, N is the density of contacts, \bar{l} is the average spacing of the centroids of contacting granules (it is basically the average grain size), and $\Omega_{1/2}$ is the surface of a half-unit sphere.

For the tractions $\bar{\mathbf{t}}^{(\mathbf{v})}$, the sign convention is shown in Fig. 1(a). At a typical contact, there are two contact forces, $\hat{\mathbf{f}}$ and $-\hat{\mathbf{f}}$, and two contact normals, \mathbf{n} and $-\mathbf{n}$. Choose the pair which points in the positive \mathbf{v} -direction. The normal tractions are then positive in *tension*. Here, each such unit normal vector represents a class of contacts, having an associated average contact force, $\hat{\mathbf{f}}$; see Mehrabadi et al. (1993). The distribution of these contact normals and forces, is thus continuous. Since the contact forces are never tensile, any chosen pair of \mathbf{n} and $\hat{\mathbf{f}}$ corresponds to negative normal tractions acting on the \mathbf{v} -plane.

3. A two-dimensional model

Consider two-dimensional deformation of a granular mass. Let $\hat{f} = \mathbf{n} \cdot \hat{\mathbf{f}}$. From Eq. (2b), the hydrostatic tension becomes

$$\frac{1}{2} \text{tr} \bar{\boldsymbol{\sigma}} = \frac{N\bar{l}}{\pi} \int_0^\pi \{1 + \mathcal{E} \cos(2\theta - 2\theta_0)\} \hat{f} \, d\theta = \frac{1}{2} N\bar{l} \hat{f}^* \quad (3a,b)$$

where \hat{f}^* is some suitable intermediate value of $\hat{f}(\theta)$ for $0 < \theta < \pi$. The pressure p is therefore given by

$$p = -\frac{1}{2} N\bar{l} \hat{f}^* \quad (4)$$

Since it is difficult to obtain an explicit expression for the contact force $\hat{\mathbf{f}}$, consider the following alternative approach. Divide $\bar{\tau}_r$, the resistance to sliding in the \mathbf{s} -direction, into two parts, one due to a Coulomb-type isotropic frictional resistance, given by $\frac{1}{2} p \sin 2\phi_\mu$, and the other due to the fabric anisotropy, denoted by $\bar{\tau}_{\text{fab}}$, where ϕ_μ is an *effective* friction angle associated with the *sliding and rolling* of granules relative to one another. To obtain an expression for τ_{fab} , use the second-order distribution density function, $E(\mathbf{n})$, given by Eq. (1a), and, as a simplest model, let $\hat{\mathbf{f}}$ be in the \mathbf{n} -direction,³ i.e., set $\hat{\mathbf{f}} \equiv \hat{\sigma} \mathbf{n}$ and from (2b) obtain

$$\bar{\boldsymbol{\sigma}} = \frac{N\bar{l}}{\pi} \int_0^\pi [1 + \mathcal{E} \cos(2\theta - 2\theta_0)] \mathbf{n} \otimes \mathbf{n} \, d\theta. \quad (5a)$$

To estimate the resisting shear stress due to fabric anisotropy, set

³ See Mehrabadi et al. (1982) for comments.

$$\begin{aligned} \bar{\tau}_{\text{fab}} &= \mathbf{v} \cdot \bar{\boldsymbol{\sigma}} \cdot \mathbf{s} = \frac{N\bar{l}}{\pi} \int_0^\pi \{1 + \mathcal{E} \cos(2\theta - 2\theta_0)\} \cos \theta \sin \theta \hat{\sigma} \, d\theta \\ &= \frac{N\bar{l}\hat{\sigma}^*}{4} \mathcal{E} \sin 2\theta_0 = -\frac{1}{2} p \hat{\mu} \mathcal{E} \sin 2\theta_0, \end{aligned} \tag{5b-f}$$

$$\hat{\mu} = \frac{\hat{\sigma}^*}{\hat{f}^*},$$

where $\hat{\sigma}^*$ is some suitable intermediate value of $\hat{\sigma}(\theta)$ for $0 < \theta < \pi$.

The resistance to sliding due to fabric is *negative* when the angle θ_0 is between 0 and $\pi/2$; see Fig. 2. In this case, the orientation of the maximum density of contact normals, i.e., the principal direction of the fabric tensor \mathcal{E} , makes an acute angle with the sliding direction \mathbf{s} . For $\frac{\pi}{2} < \theta_0 < \pi$, on the other hand, both the overall friction and the fabric anisotropy contribute to the resistance to sliding. The total resistance to sliding therefore is

$$\bar{\tau}_r = \frac{1}{2} p \sin \phi_\mu - \frac{1}{2} p \hat{\mu} \mathcal{E} \sin 2\theta_0. \tag{6}$$

The second term on the right-hand side of (6) is the shear component of the tensor, $-\frac{1}{2} p \hat{\mu} \mathcal{E}$, on the \mathbf{s} -direction. In view of this, introduce a deviatoric *anisotropy tensor (backstress)*,

$$\boldsymbol{\beta} \equiv -\frac{1}{2} p \hat{\mu} \mathcal{E} \tag{7}$$

with the following properties:

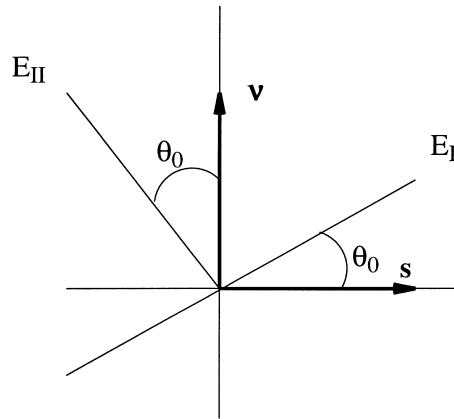


Fig. 2. The angle θ_0 measures the orientation of the major principal axis of the fabric tensor \mathcal{E} from the sliding direction, \mathbf{s} ; the greatest density of contact normals is along this principal orientation, associated with the principal value $E_I \geq 0$.

$$\left(\frac{1}{2}\beta_{ij}\beta_{ij}\right)^{1/2} = \beta = \frac{1}{2}p\hat{\mu}\mathcal{E}, \quad \tan 2\nu_0 = \frac{2\beta_{12}}{\beta_{11} - \beta_{22}}, \quad \beta_{22} = -\beta_{11},$$

$$\beta_{11} = \beta \cos 2\nu_0, \quad \beta_{12} = \beta \sin 2\nu_0, \quad \nu_0 = \theta_0 \pm \frac{\pi}{2}. \quad (8a-f)$$

The major principal axis of $\boldsymbol{\beta}$ coincides with the minor principal axis of \mathcal{E} . The major principal value β_I of $\boldsymbol{\beta}$, therefore, corresponds to the least density of contact normals, or the maximum dilatancy direction. This direction makes an angle ν_0 with the sliding direction, \mathbf{s} . For $0 < \nu_0 < \frac{\pi}{2}$, the resistance to sliding due to fabric, $\bar{\tau}_{\text{fab}}$, is *positive*, whereas for $\frac{\pi}{2} < \nu_0 < \pi$, it is *negative*. In the first case, sliding in the positive \mathbf{s} -direction is accompanied by *dilatancy*, while in the second case, it is accompanied by *densification*.

4. Meso-scale yield condition

Consider a typical sliding plane at the meso-scale. The resistance to shearing of the granules over this plane is due to interparticle friction and fabric anisotropy, as is expressed by (6). The micromechanical formulation of the preceding subsection provides explicit expressions for the parameters which define this resistance. The resulting quantities, ϕ_μ , $\boldsymbol{\beta}$, β , and ν_0 , have physical meanings, and are related to the microstructure of the granular mass. Hence, they can be associated with the continuum field variables. In Eq. (6), p is the pressure, externally applied to the granular mass, and ϕ_μ is the overall effective friction angle which can be measured and experimentally related to the void ratio and the interparticular properties.⁴ The quantities β and ν_0 characterize the fabric anisotropy, and their evolution may be defined by rate constitutive equations.

Based on expression (6), consider the following sliding criterion, a variant of Coulomb's criterion, for the sliding in the \mathbf{s} -direction, over a plane with unit normal \mathbf{v} :

$$f \equiv \tau_v - \frac{1}{2}p \sin 2\phi_\mu - \beta \sin 2\nu_0 \leq 0. \quad (9a)$$

The shear, τ_v , and normal, σ_v , stresses acting on the \mathbf{s} -plane, as well as the pressure, p , are given by

$$\tau_v = \boldsymbol{\tau}:(\mathbf{v} \otimes \mathbf{s}), \quad \sigma_v = \boldsymbol{\tau}:(\mathbf{v} \otimes \mathbf{v}) < 0, \quad p = -\frac{1}{2}\text{tr}(\boldsymbol{\tau}), \quad (9b-d)$$

⁴ High strain-rate deformations of confined frictional granules produce considerable heat at interparticle contact points, which may lead to melting of the interface material. The friction angle ϕ_μ then depends on the interface temperature which in turn is a function of the deformation history. Effects of this kind can be included in the model.

where $\boldsymbol{\tau}$ is the Kirchhoff stress.⁵ Here and in the sequel, the usual continuum mechanics sign convention is used, so that *tension is regarded positive*.

In Eq. (9a), the first term is the driving shear stress. The other two terms denote the resistance due to the interparticle (isotropic) friction, and the fabric anisotropy, respectively. The shear resistance due to fabric anisotropy is a function of the angle between the sliding plane and the principal axes of the fabric tensor, as well as a function of the anisotropy parameter β . In Eq. (9c), the normal stress σ_v is assumed to be compressive, since frictional granules cannot sustain tension.

In view of (9a), consider a decomposition of the Kirchhoff stress tensor $\boldsymbol{\tau}$ into three parts, as follows:

$$\boldsymbol{\tau} = \mathbf{S} - p\mathbf{1} + \boldsymbol{\beta}, \quad (10a)$$

where the backstress, $\boldsymbol{\beta}$, defined by ((7) and (8a)), and *the stress-difference*, \mathbf{S} , are *deviatoric* and symmetric tensors, and $\mathbf{1}$ is the second-order identity tensor. Let the principal values of these tensors be denoted by β_i and S_i , $i = \text{I, II}$, and assume that S_{I} and β_{I} make angles θ and ν_0 with the sliding direction, \mathbf{s} . In view of Eqs. (10a) and (9b), the resolved shear stress on the sliding direction is given by

$$\tau_v = S \sin 2\theta + \beta \sin 2\nu_0, \quad S = \left(\frac{1}{2} \mathbf{S} : \mathbf{S} \right)^{1/2}. \quad (10b,c)$$

The sliding condition (9a) now becomes

$$f \equiv S \sin 2\theta - \frac{1}{2} p \sin 2\phi_\mu \leq 0. \quad (11a)$$

The sliding occurs on planes for which (11a) attains its maximum value of zero,

$$S = p \sin \phi_\mu. \quad (11b)$$

There are two planes for which (11b) is satisfied. These are given by $\theta = \pm(\frac{\pi}{4} + \frac{\phi_\mu}{2})$. These planes are situated symmetrically about the greater principal stress, S_{I} (see Fig. 3), making an angle $\frac{\pi}{4} + \frac{\phi_\mu}{2}$ with this direction. The decomposition of the stress tensor $\boldsymbol{\tau}$ may be implemented as follows.

In the x_1, x_2 -plane, identify the angle θ_E of the orientation of the *minor* principal value, E_{II} , of the fabric tensor \mathcal{E} , relative to the x_1 -direction; see Fig. 3. This corresponds to the minimum density of the contact unit normals, and coincides with the *major* principal direction of $\boldsymbol{\beta}$. Denote by the unit vectors $\hat{\mathbf{e}}_i$, $i = 1, 2$, the principal directions of $\boldsymbol{\beta}$. Then, this tensor is given by

⁵ The Kirchhoff stress is used in place of the Cauchy stress. When the current configuration is used as the reference one, the Cauchy and Kirchhoff stresses coincide (but not their rates).

$$\boldsymbol{\beta} = \beta(\hat{\mathbf{e}}_1 \otimes \hat{\mathbf{e}}_1 - \hat{\mathbf{e}}_2 \otimes \hat{\mathbf{e}}_2), \quad \beta_I = -\beta_{II} = \beta = \frac{1}{2}p\hat{\mu}\mathcal{E} \geq 0. \tag{12a,b}$$

The tensor \mathbf{S} is thus obtained from

$$\mathbf{S} = \boldsymbol{\tau}' - \boldsymbol{\beta}, \tag{12c}$$

where prime denotes the deviatoric part. Fig. 3 shows the S_I -axis and the corresponding two sliding planes, \mathbf{s}^i , $i = 1, 2$, together with the corresponding unit normals, \mathbf{n}^i . The S_I -axis makes an angle ψ with the x_1 -axis. Because of the sign convention, $S_I > 0$ (tension) and $S_{II} < 0$ (compression). The sliding directions are shown by arrows in this figure.

The decomposition (10a) can be interpreted in terms of the continuum plasticity models. The tensor $\boldsymbol{\beta}$, which is proportional to the pressure p , represents the kinematic hardening. The tensor \mathbf{S} , with $S \leq p \sin \phi_\mu$, is the yield circle in the deviatoric stress space; see Fig. 4, where $\boldsymbol{\mu} = \frac{\mathbf{S}}{\sqrt{2}S}$ is a unit tensor normal to the yield circle. Unlike for metals, the origin of the coordinates in this space, can fall outside the yield circle.

For each sliding plane, both isotropic and kinematic hardening may occur. The

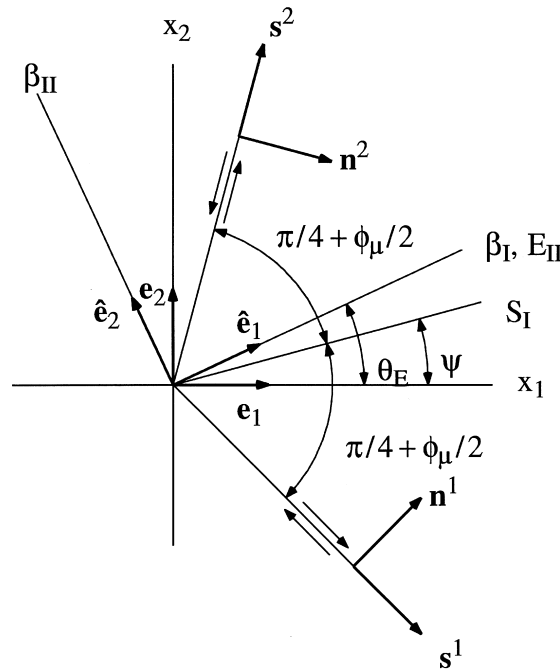


Fig. 3. To decompose the deviatoric part, $\boldsymbol{\tau}'$, of the stress tensor $\boldsymbol{\tau}$: (1) identify the angle θ_E of the direction of the minor principal axis, E_{II} , of the fabric tensor, \mathcal{E} , relative to the x_1 -axis; (2) measure from the x_1 -axis an angle θ_E to the direction $\hat{\mathbf{e}}_1$ of β_I , as shown; (3) then $\mathbf{S} = \boldsymbol{\tau}' - \boldsymbol{\beta}$, and sliding directions with unit vectors \mathbf{s}^1 and \mathbf{s}^2 , form angles $\pm(\frac{\pi}{4} + \frac{\phi_\mu}{2})$ with the major principal axis, S_I , which makes angle ψ with the x_1 -axis; the pair of unit vectors \mathbf{s}^α and \mathbf{n}^α , $\alpha = 1, 2$, form a sliding system.

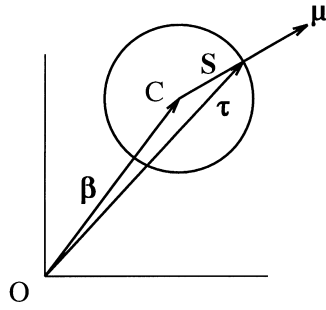


Fig. 4. Yield surface in deviatoric stress space; $\mu = S/(\sqrt{2}S)$ is a unit tensor normal to the yield circle.

isotropic hardening (softening) is due to densification (dilatancy), and kinematic hardening is due to redistribution of contact normals, being measured by the fabric tensor \mathcal{E} or, equivalently, by β .

During the course of deformation, the fabric and the void ratio change. As the fabric changes, the center of the yield circle moves in the deviatoric stress space. This corresponds to *kinematic hardening*. On the other hand, the effective friction angle, ϕ_μ , which represents the effective interparticle friction at the meso-scale, changes with the void ratio, resulting in a change in the radius of the yield surface. This corresponds to isotropic hardening or softening. As the void ratio increases, the interaction of particles decreases and hence the shear resistance decreases (softening), whereas a decrease in the void ratio corresponds to an increase in the shear resistance (hardening). The isotropic softening during the dilatancy phase of the deformation, is generally accompanied by an anisotropic hardening due to the redistribution of the contact normals, resulting in an increase in their density in the direction of maximum compression.

5. Loading and unloading

It is known that *unloading* from an anisotropic state may produce *reverse inelastic deformation, even against an applied shear stress*; see Nemat-Nasser (1980) and Okada and Nemat-Nasser (1994). Furthermore, in a continued monotonic deformation, the principal axes of the stress and the fabric tensors tend to coincide.

Consider the biaxial loading shown in Fig. 5, and assume that the loading has induced a strong anisotropy, with $\beta \approx S$. The sliding directions in loading make angles of $\pm(\frac{\pi}{4} + \frac{\phi_\mu}{2})$ with the S_I -direction. These directions are identified in Fig. 5 by the term *loading*.

Suppose that an unloading is now initiated by the addition of an incremental shear stress $\Delta\tau_{11} = -\Delta S$ (compression) in the S_I -direction and $\Delta\tau_{22} = \Delta S$ (tension) in the S_{II} -direction, where $\Delta S > 0$. Reverse plastic deformation is possible on the sliding planes denoted by the term *unloading* in Fig. 5. These planes make angles

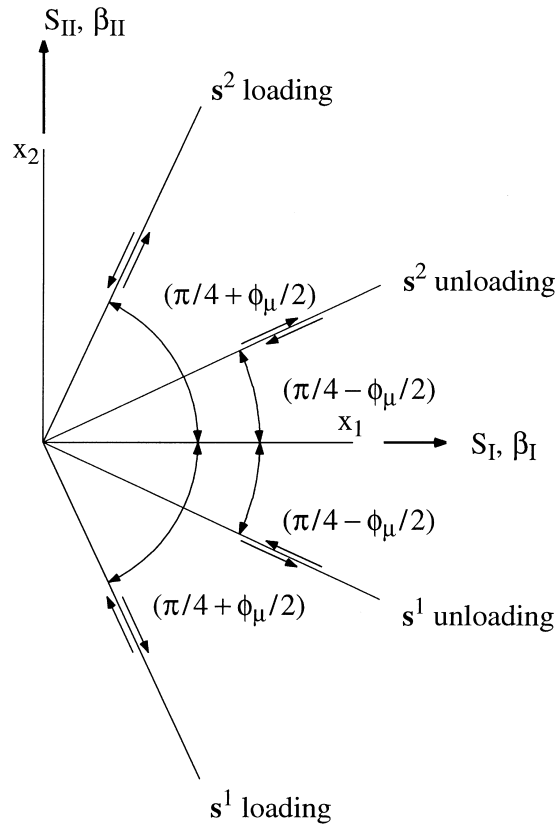


Fig. 5. Sliding planes in loading and unloading: in biaxial loading, the stress state is given by $\tau_{11} = -p + S + \beta$ and τ_{22} ; in unloading, the driving shear stress is defined by $\Delta\tau_{11} = -\Delta S - \beta$ and $\Delta\tau_{22} = \Delta S + \beta$ which may produce reverse plastic deformation, where $\Delta S > 0$ is the unloading shear stress increment.

$\pm(\frac{\pi}{4} - \frac{\phi_{\mu}}{2})$ with the S_I -direction. It is important to note that, at the inception of unloading, the granular mass is in equilibrium, having a highly biased fabric. The unloading from this state is equivalent to the reverse incremental loading with the fabric now assisting the corresponding reverse deformation. Densification accompanies this reverse loading. The required energy is supplied by the work of the applied pressure going through the volumetric contraction.

6. A rate-independent compressible double-sliding model

The meso-scale double-sliding formulation of the preceding section will now be used to develop a model for planar deformation of frictional granules, similar to that of crystals. To this end, assume that the total plastic deformation at the

continuum level, consists of two superimposed shearing deformations along the active sliding planes. This sliding is accompanied by volumetric changes and induced anisotropy. Based on these concepts, a complete set of constitutive relations is produced in what follows.

6.1. Kinematics

The aim is to obtain continuum constitutive relations implied by the double-sliding theory, in line with the deformation mechanism discussed in the preceding sections. Let, at the continuum level, the kinematics of instantaneous granular deformation be expressed by the velocity gradient $\mathbf{L} = (\frac{\partial \mathbf{v}}{\partial \mathbf{x}})^T$, consisting of a symmetric part, \mathbf{D} , the deformation rate tensor, and an antisymmetric part, \mathbf{W} , the spin tensor. Each of these rates is separated into elastic and plastic parts as follows:

$$\mathbf{D} = \mathbf{D}^* + \mathbf{D}^p, \quad \mathbf{W} = \mathbf{W}^* + \mathbf{W}^p, \quad (13a,b)$$

where superscript p denotes the plastic part which is due to shearing along the sliding directions, and superscript * denotes the elastic part; note that \mathbf{W}^* also includes the rigid-body spin.

As shown in Fig. 3, in plane flow, there are two preferred sliding planes, symmetrically situated about the principal directions of the stress-difference, \mathbf{S} . The first, the \mathbf{s}^1 -direction, makes an angle $\theta^1 = \psi - \frac{\pi}{4} \mp \frac{\phi_\mu}{2}$, and the second, the \mathbf{s}^2 -direction, makes an angle $\theta^2 = \psi + \frac{\pi}{4} \pm \frac{\phi_\mu}{2}$, with the positive x_1 -axis; here and in the sequel, the upper and lower signs correspond to loading and unloading, respectively. Assuming that the plastic deformation is due to shearing on the sliding planes, and denoting the rate of shearing in the *positive* \mathbf{s}^α -sliding direction by $\dot{\gamma}^\alpha$ ($\alpha = 1, 2$), write the plastic part of the velocity gradient as

$$\mathbf{D}^p = \sum_{\alpha=1}^2 \pm \dot{\gamma}^\alpha \mathbf{p}^\alpha, \quad \mathbf{W}^p = \sum_{\alpha=1}^2 \pm \dot{\gamma}^\alpha \mathbf{r}^\alpha, \quad (14a,b)$$

where the negative sign denotes sliding in the *negative* direction of the \mathbf{s}^α -axis (unloading), and the second-order tensors \mathbf{p}^α and \mathbf{r}^α are defined by

$$\mathbf{p}^\alpha = \frac{1}{2}(\mathbf{s}^\alpha \otimes \mathbf{n}^\alpha + \mathbf{n}^\alpha \otimes \mathbf{s}^\alpha) \pm \mathbf{n}^\alpha \otimes \mathbf{n}^\alpha \tan \delta^\alpha, \\ \mathbf{r}^\alpha = \frac{1}{2}(\mathbf{s}^\alpha \otimes \mathbf{n}^\alpha - \mathbf{n}^\alpha \otimes \mathbf{s}^\alpha). \quad (15a,b)$$

Here δ^α , $\alpha = 1, 2$, are the dilatancy angles associated with the sliding planes, as shown in Fig. 3. They represent the orientation of the effective microscopic planes of motion relative to the corresponding mesoscopic sliding planes.

The vectors \mathbf{s}^α and \mathbf{n}^α are unit vectors in the positive direction of the sliding and normal to the plane of sliding, respectively. The α th sliding plane and the sliding

direction on this plane form a *sliding system*. In the double-sliding model, there are two such systems which can be activated simultaneously. In each sliding direction, the sliding rate is positive for loading and negative for unloading. The unit vectors are defined by

$$\begin{aligned} \mathbf{s}^1 &= \{\cos \theta^1, \sin \theta^1\}, & \mathbf{n}^1 &= \{-\sin \theta^1, \cos \theta^1\}, \\ \mathbf{s}^2 &= \{\cos \theta^2, \sin \theta^2\}, & \mathbf{n}^2 &= \{\sin \theta^2, -\cos \theta^2\}, \end{aligned} \quad (16a-d)$$

where

$$\begin{aligned} \theta^1 + \theta^2 &= 2\psi, & \theta^2 - \theta^1 &= \frac{\pi}{2} \pm \phi_\mu, & \tan 2\psi &= \frac{2S_{12}}{S_{11} - S_{22}}, \\ S_{22} &= -S_{11}, & S &= \left(\frac{1}{2}S_{ij}S_{ij}\right)^{1/2}. \end{aligned} \quad (17a-e)$$

6.2. Plastic deformation rate

In what follows, alternative representations of the plastic strain rate tensor, \mathbf{D}^p , are given in terms of the friction angle, ϕ_μ , dilatancy parameters, δ^α , $\alpha = 1, 2$, the orientation, ψ , of the major principal stress, S_1 , and the slip rates, $\dot{\gamma}^\alpha$.

6.3. Notation

To simplify the expressions, only the loading-induced deformation is considered. To obtain the corresponding expressions for unloading, simply reverse the signs of ϕ_μ , δ^α and $\dot{\gamma}^\alpha$, in the corresponding expressions.

7. Constitutive relations for double-sliding model

To complete the constitutive relations, two ingredients are necessary. These are: (1) the elasticity relations; and (2) the evolutionary equation for the variation of the fabric tensor $\boldsymbol{\beta}$. Once these two ingredients are provided, then the slip rates can be computed using the yield and the *consistency* conditions.

7.1. Yield and consistency conditions

The yield condition, given by (9a), applies to each sliding system. Introduce the notation

$$\mathbf{q}^\alpha = \frac{1}{2}(\mathbf{s}^\alpha \otimes \mathbf{n}^\alpha + \mathbf{n}^\alpha \otimes \mathbf{s}^\alpha) + \mathbf{n}^\alpha \otimes \mathbf{n}^\alpha \tan \phi_\mu,$$

$$\mathbf{d}^\alpha = \frac{1}{2}(\mathbf{s}^\alpha \otimes \mathbf{n}^\alpha + \mathbf{n}^\alpha \otimes \mathbf{s}^\alpha), \quad (18a,b)$$

and observe that the yield condition (9a) then gives

$$\tau^\alpha + \sigma^\alpha \tan \phi_\mu = \boldsymbol{\beta} : \mathbf{d}^\alpha, \quad \alpha = 1, 2, \quad (19a)$$

where $\tau^\alpha = \boldsymbol{\tau} : \mathbf{d}^\alpha$ and $\sigma^\alpha = \boldsymbol{\tau} : (\mathbf{n}^\alpha \otimes \mathbf{n}^\alpha)$ are the resolved shear stress and the normal stress acting on the α th sliding plane. In view of (18), the yield condition becomes

$$\boldsymbol{\tau} : \mathbf{q}^\alpha = \boldsymbol{\beta} : \mathbf{d}^\alpha. \quad (19b)$$

The consistency condition is obtained from the requirement that, for continued plastic flow, the stress point must remain on the yield surface associated with each sliding plane. Denote the rigid-body spin of the sliding systems by \mathbf{W}^* . It then follows that the time variation of the unit vectors \mathbf{n}^α and \mathbf{s}^α are defined by

$$\dot{\mathbf{n}}^\alpha = \mathbf{W}^* \mathbf{n}^\alpha, \quad \dot{\mathbf{s}}^\alpha = \mathbf{W}^* \mathbf{s}^\alpha, \quad (20a,b)$$

where

$$W_{12}^* = -W_{21}^* = W_{12} - W_{12}^p \quad (20c)$$

Direct calculations⁶ now show that $\dot{\tau}^\alpha = \overset{\circ}{\boldsymbol{\tau}}^* : \mathbf{d}^\alpha$ and $\dot{\sigma}^\alpha = \overset{\circ}{\boldsymbol{\tau}}^* : (\mathbf{n}^\alpha \otimes \mathbf{n}^\alpha)$, where

$$\overset{\circ}{\boldsymbol{\tau}}^* = \dot{\boldsymbol{\tau}} - \mathbf{W}^* \boldsymbol{\tau} + \boldsymbol{\tau} \mathbf{W}^* \quad (21a)$$

is the Jaumann rate of the Kirchhoff stress, corotational with the sliding systems. Hence, taking the time derivative of both sides of (19a), it follows that

$$\overset{\circ}{\boldsymbol{\tau}}^* : \mathbf{q}^\alpha = \overset{\circ}{\boldsymbol{\beta}}^* : \mathbf{d}^\alpha, \quad (21b)$$

where the Jaumann rate $\overset{\circ}{\boldsymbol{\beta}}^*$ is defined by

$$\overset{\circ}{\boldsymbol{\beta}}^* = \dot{\boldsymbol{\beta}} - \mathbf{W}^* \boldsymbol{\beta} + \boldsymbol{\beta} \mathbf{W}^*. \quad (21c)$$

7.2. Fabric evolution

The fabric changes with the continued plastic flow of the granular mass. This change must be quantified in terms of the deformation or stress measures. Experimental observations of the photoelastic granules⁷ suggest that the fabric changes with the stress, tending to become coaxial with it. On the other hand, the same experimental results show that, it may be equally reasonable to assume that the fabric tensor changes with the plastic straining. This is then more in line with classical plasticity; see Hill (1950). Hence, consider the following rule for the rate

⁶ See Nemat-Nasser et al. (1981).

⁷ See Mehrabadi et al. (1988) and Oda et al. (1982)

of change of the fabric tensor $\boldsymbol{\beta}$:

$$\dot{\boldsymbol{\beta}}^* = A\mathbf{D}^p, \quad (22)$$

where A is a material function.

7.3. Elasticity relations

The general elasticity relations⁸ are used as the starting point. Then they are simplified by invoking relevant symmetries, as necessary. To this end, consider the instantaneous elastic modulus tensor \mathcal{L} and decompose it into its deviatoric and spherical parts, as follows:

$$\begin{aligned} \mathcal{L} &= \mathcal{L}' + \frac{1}{2}(\mathbf{N} \otimes \mathbf{1} + \mathbf{1} \otimes \mathbf{N}) - \frac{\kappa}{4}\mathbf{1} \otimes \mathbf{1} \\ &= \mathcal{L}' + \frac{1}{2}(\mathbf{N}' \otimes \mathbf{1} + \mathbf{1} \otimes \mathbf{N}') + \frac{\kappa}{4}\mathbf{1} \otimes \mathbf{1}, \end{aligned} \quad (23a,b)$$

where

$$\begin{aligned} \mathcal{L}'_{iikl} = \mathcal{L}'_{klij} = 0, \quad \mathbf{N}_{ij} = \mathcal{L}_{ijkk} = \mathcal{L}_{kkij}, \\ \mathbf{N} = \mathbf{N}' + \frac{\kappa}{2}\mathbf{1}, \quad \kappa = \text{tr}(\mathbf{N}) = \mathcal{L}_{ijij} \quad i, j, k, l = 1, 2, \end{aligned} \quad (23c-f)$$

where prime denotes the deviatoric part.

The elastic part of the deformation rate tensor is now expressed in terms of the Jaumann rate of change of the Kirchhoff stress, corotational with the sliding systems, $\hat{\boldsymbol{\tau}}^*$, as follows:

$$\hat{\boldsymbol{\tau}}^* = \mathcal{L}:\mathbf{D}^e = \mathcal{L}:(\mathbf{D} - \mathbf{D}^p). \quad (24a,b)$$

For frictional granular materials, the elasticity tensor \mathcal{L} , in general, is not constant, but rather, it depends on the fabric tensor. When the distribution of the contact unit normals is represented by a second-order tensor, then it is reasonable to assume an orthotropic elasticity tensor with the axes of orthotropy defined by the principal axes of the fabric tensor, $\boldsymbol{\beta}$. Hence, in the $\hat{\mathbf{e}}_i$ -coordinate system of Fig. 3, the elastic response is expressed as

$$\begin{aligned} \hat{\tau}_{11}^* &= C_{11}\hat{D}_{11}^* + C_{12}\hat{D}_{22}^*, & \hat{\tau}_{22}^* &= C_{12}\hat{D}_{11}^* + C_{22}\hat{D}_{22}^*, \\ \hat{\tau}_{12}^* &= C_{33}\hat{D}_{12}^*, \end{aligned} \quad (25a-c)$$

where superposed $\hat{}$ is used to denote the tensor components in the principal axes

⁸ See Nemat-Nasser and Hori (1993).

of the fabric tensor. These equations can be rewritten in tensor form as,

$$\begin{aligned} \overset{\circ}{\tau}_{kk}^* &= 2KD_{kk}^* + 2\sqrt{2}\bar{K}(\boldsymbol{\mu}_\beta:\mathbf{D}^*), \\ \overset{\circ}{\tau}^{*'} &= \sqrt{2}\bar{K}D_{kk}^*\boldsymbol{\mu}_\beta + 2G\mathbf{D}^{*'} + 2\bar{G}(\boldsymbol{\mu}_\beta:\mathbf{D}^*)\boldsymbol{\mu}_\beta, \end{aligned} \tag{26a,b}$$

where $\boldsymbol{\mu}_\beta$ is the unit fabric tensor, defined by

$$\boldsymbol{\mu}_\beta = \frac{\hat{\mathbf{e}}_1 \otimes \hat{\mathbf{e}}_1 - \hat{\mathbf{e}}_2 \otimes \hat{\mathbf{e}}_2}{\sqrt{2}} = \frac{\boldsymbol{\beta}}{\sqrt{2}\boldsymbol{\beta}}, \tag{26c}$$

and the other parameters are given in terms of C_{ij} by

$$\begin{aligned} K &= \frac{C_{11} + C_{22} + 2C_{12}}{4}, \quad \bar{K} = \frac{C_{11} - C_{22}}{4}, \\ G &= \frac{C_{33}}{2}, \quad \bar{G} = \frac{C_{11} + C_{22} + 2C_{12}}{4}. \end{aligned} \tag{26d–g}$$

In view of (23a,b), it follows that

$$\begin{aligned} \mathcal{L}' &= 2G\left(\mathbf{1}^{(4s)} - \frac{1}{2}\mathbf{1} \otimes \mathbf{1}\right) + 2\bar{G}\boldsymbol{\mu}_\beta \otimes \boldsymbol{\mu}_\beta, \quad N' = 2\sqrt{2}\bar{K}\boldsymbol{\mu}_\beta, \quad \kappa = 4K, \\ \mathcal{L} &= 2G\left(\mathbf{1}^{(4s)} - \frac{1}{2}\mathbf{1} \otimes \mathbf{1}\right) + 2\bar{G}\boldsymbol{\mu}_\beta \otimes \boldsymbol{\mu}_\beta + \sqrt{2}\bar{K}(\boldsymbol{\mu}_\beta \otimes \mathbf{1} + \mathbf{1} \otimes \boldsymbol{\mu}_\beta) + K\mathbf{1} \\ &\quad \otimes \mathbf{1}. \end{aligned} \tag{26h,i}$$

7.4. Calculation of sliding rates

Consider constitutive assumption (24). Then, in view of (21), (22), and (18), it follows that

$$\begin{aligned} \boldsymbol{\lambda}^\alpha:\mathbf{D} &= \sum_{\beta=1}^2 \{(\boldsymbol{\lambda}^\alpha + \Lambda\mathbf{d}^\alpha):\mathbf{p}^\beta\} \dot{\gamma}^\beta = \sum_{\beta=1}^2 h^{\alpha\beta} \dot{\gamma}^\beta, \\ h^{\alpha\beta} &= (\boldsymbol{\lambda}^\alpha + \Lambda\mathbf{d}^\alpha):\mathbf{p}^\beta, \quad \boldsymbol{\lambda}^\alpha = \mathcal{L}:\mathbf{q}^\alpha. \end{aligned} \tag{27a–d}$$

Now, with $[\mathbf{g}^{\alpha\beta}]$ denoting the inverse of $[h^{\alpha\beta}]$, obtain

$$\dot{\gamma}^\alpha = \sum_{\beta=1}^2 \mathbf{g}^{\alpha\beta} \boldsymbol{\lambda}^\beta:\mathbf{D}. \tag{27e}$$

The plastic deformation rate tensor, \mathbf{D}^p , and the plastic spin, \mathbf{W}^p , are now obtained from (14a,b).

7.5. Final constitutive relations

Expressions (14), (24) and (27e) can be combined to relate the stress rate $\dot{\boldsymbol{\tau}}$ directly to the deformation rate tensor \mathbf{D} . To this end, first note that

$$\dot{\boldsymbol{\tau}} = \mathcal{L}:\mathbf{D} - \sum_{\alpha=1}^2 \dot{\gamma}^{\alpha} \mathbf{l}^{\alpha}, \quad \mathbf{l}^{\alpha} = \mathcal{L}:\mathbf{p}^{\alpha} + \mathbf{r}^{\alpha} \boldsymbol{\tau} - \boldsymbol{\tau} \mathbf{r}^{\alpha}. \quad (28a,b)$$

Then, by direct substitution obtain

$$\dot{\boldsymbol{\tau}} = \mathcal{H}:\mathbf{D}, \quad (28c)$$

where \mathcal{H} is defined by

$$\mathcal{H} = \mathcal{L} - \sum_{\alpha, \beta=1}^2 g^{\alpha\beta} \mathbf{l}^{\alpha} \otimes \boldsymbol{\lambda}^{\beta}. \quad (28d)$$

In these expressions, the constitutive parameters which must yet be defined are δ^{α} and Λ , which, respectively, define the dilatancy and the evolution of the backstress.

7.6. Dilatancy and densification

A procedure proposed by Nemat-Nasser (1980) may be used to obtain an expression for $\tan \delta^{\alpha}$ in terms of the friction coefficient and the fabric tensor, as follows.

Consider a *virtual* sliding $\Delta\gamma^{\alpha}$ of the α th sliding system. The work done by the applied stress, $\boldsymbol{\tau}$, is given by

$$\Delta w_1 = (-p \tan \delta^{\alpha} + \boldsymbol{\tau}:\mathbf{d}^{\alpha}) \Delta\gamma^{\alpha}, \quad (29a)$$

where expansion is regarded positive. The corresponding frictional dissipation is represented by

$$\Delta w_2 = p M_f \Delta\gamma^{\alpha}, \quad (29b)$$

where M_f is the effective overall friction coefficient. From (11b), $\boldsymbol{\tau}:\mathbf{d}^{\alpha} = S \sin 2\theta + \beta \sin 2\nu_0$, where $\theta = \frac{\pi}{4} + \frac{\phi_{\mu}}{2}$, and ν_0^{α} is the angle between the direction of the major (minor) principal value β_1 (principal value E_{11}) of the fabric tensor $\boldsymbol{\beta}$ (fabric tensor \mathcal{E}) and the sliding direction. It hence follows that

$$-\tan \delta^{\alpha} = M_f - \frac{S}{p} \cos \phi_{\mu} - \frac{1}{2} \hat{\mu} \mathcal{E} \sin 2\nu_0^{\alpha}. \quad (29c)$$

For an initially isotropic sample, $\mathcal{E} = 0$, the right-hand side of (29c) is initially positive, leading to initial densification. As the deformation proceeds, the second and third terms in the right-hand side increase in absolute value, eventually leading to dilatancy in continued loading. Unloading from such a state can now produce extensive densification. Since the yield condition (11b) must be satisfied for sliding to occur, $S = p \sin \phi_\mu$, and

$$\tan \delta^z = -M_f + \frac{1}{2} \sin 2\phi_\mu + \frac{1}{2} \hat{\mu} \mathcal{E} \sin 2\nu_0^z. \quad (29d)$$

This is an important ingredient of the theory. It couples the dilatancy with the friction and the fabric of the granular mass. According to this equation, continued monotonic deformation is accompanied by dilatancy, and subsequent unloading, by densification.

The material functions A , ϕ_μ , and M_f must be obtained in terms of the void ratio and the characteristics of the granules, empirically; for special cases, see Nemat-Nasser and Shokoh (1980) and Balendran and Nemat-Nasser (1993a). Similarly, the elasticity parameters C_{ij} in (25a–c) must be related to the microstructure and must be measured.

8. A continuum model based on double sliding

Start with definition (14a,b), and noting (17a–e), obtain the following relations for the components of the plastic part of the velocity gradient, $\mathbf{L}^p = \mathbf{D}^p + \mathbf{W}^p$:

$$D_{kk}^p = (\dot{\gamma}^1 \tan \delta^1 + \dot{\gamma}^2 \tan \delta^2), \quad W_{12}^p = \frac{1}{2} (\dot{\gamma}^1 - \dot{\gamma}^2),$$

$$D_{11}^{p'} = \frac{1}{2} \dot{\gamma}^1 \frac{\cos(2\psi - (\phi_\mu - \delta^1))}{\cos \delta^1} + \frac{1}{2} \dot{\gamma}^2 \frac{\cos(2\psi + (\phi_\mu - \delta^2))}{\cos \delta^2} = -D_{22}^{p'},$$

$$D_{12}^p = \frac{1}{2} \dot{\gamma}^1 \frac{\sin(2\psi - (\phi_\mu - \delta^1))}{\cos \delta^1} + \frac{1}{2} \dot{\gamma}^2 \frac{\sin(2\psi + (\phi_\mu - \delta^2))}{\cos \delta^2}. \quad (30a-e)$$

In terms of the components of the stress-difference tensor, \mathbf{S} , the deviatoric components of the deformation rate tensor can be rewritten as

$$\begin{aligned}
D_{11}^{p'} &= \frac{S_{11}}{2S} \left\{ \dot{\gamma}^1 \frac{\cos(\phi_\mu - \delta^1)}{\cos \delta^1} + \dot{\gamma}^2 \frac{\cos(\phi_\mu - \delta^2)}{\cos \delta^2} \right\} + \frac{S_{12}}{2S} \left\{ \dot{\gamma}^1 \frac{\sin(\phi_\mu - \delta^1)}{\cos \delta^1} \right. \\
&\quad \left. - \dot{\gamma}^2 \frac{\sin(\phi_\mu - \delta^2)}{\cos \delta^2} \right\}, \\
D_{12}^p &= \frac{S_{12}}{2S} \left\{ \dot{\gamma}^1 \frac{\cos(\phi_\mu - \delta^1)}{\cos \delta^1} + \dot{\gamma}^2 \frac{\cos(\phi_\mu - \delta^2)}{\cos \delta^2} \right\} \\
&\quad - \frac{S_{11}}{2S} \left\{ \dot{\gamma}^1 \frac{\sin(\phi_\mu - \delta^1)}{\cos \delta^1} - \dot{\gamma}^2 \frac{\sin(\phi_\mu - \delta^2)}{\cos \delta^2} \right\}. \tag{31a,b}
\end{aligned}$$

It is seen that the deviatoric plastic deformation rate tensor, $\mathbf{D}^{p'}$, is *not* coaxial with the stress-difference tensor, \mathbf{S} , unless $\delta^1 = \delta^2 = \phi_\mu$, or in special cases, when $\dot{\gamma}^1 = \dot{\gamma}^2$ and $\delta^1 = \delta^2$.

To relate the double-sliding model to the continuum models, consider Eqs. (31a,b), and introduce the notation

$$A^\alpha = \frac{\cos(\phi_\mu - \delta^\alpha)}{\cos \delta^\alpha}, \quad B^\alpha = \frac{\sin(\phi_\mu - \delta^\alpha)}{\cos \delta^\alpha}, \quad \alpha = 1, 2. \tag{32a,b}$$

Then set

$$\dot{\gamma} = \dot{\gamma}^1 A^1 + \dot{\gamma}^2 A^2, \quad \dot{\omega} = \dot{\gamma}^1 B^1 - \dot{\gamma}^2 B^2, \tag{33a,b}$$

and note that $\dot{\gamma}^1$ and $\dot{\gamma}^2$ are given by

$$\dot{\gamma}^1 = \frac{\dot{\gamma} B^2 + \dot{\omega} A^2}{A^1 B^2 + A^2 B^1}, \quad \dot{\gamma}^2 = \frac{\dot{\gamma} B^1 - \dot{\omega} A^1}{A^1 B^2 + A^2 B^1}. \tag{33c,d}$$

It is convenient to use $\dot{\gamma}$ and $\dot{\omega}$ instead of the sliding rates, $\dot{\gamma}^1$ and $\dot{\gamma}^2$. When $\delta^1 = \delta^2$, then $\dot{\gamma}$ is proportional to $\dot{\gamma}^1 + \dot{\gamma}^2$ and $\dot{\omega}$ is proportional to the plastically-induced spin, $\frac{1}{2}(\dot{\gamma}^1 - \dot{\gamma}^2)$. All quantities which describe the plastic deformation rate can be expressed in terms of $\dot{\gamma}$ and $\dot{\omega}$. In particular, (19) reduces to

$$D_{11}^{p'} = \dot{\gamma} \frac{S_{11}}{2S} + \dot{\omega} \frac{S_{12}}{2S}, \quad D_{12}^p = \dot{\gamma} \frac{S_{12}}{2S} - \dot{\omega} \frac{S_{11}}{2S}, \tag{34a,b}$$

and (30a,b) become

$$D_{kk}^p = \dot{\gamma} \Gamma + \dot{\omega} \Omega, \quad W_{12}^p = \dot{\gamma} \frac{B^2 - B^1}{2\Delta} + \dot{\omega} \frac{A^2 + A^1}{2\Delta}, \tag{34c,d}$$

where

$$\Delta = A^1 B^2 + A^2 B^1 = \frac{\sin(2\phi_\mu - (\delta^1 + \delta^2))}{\cos \delta^1 \cos \delta^2},$$

$$\Gamma = \frac{B^2 \tan \delta^1 + B^1 \tan \delta^2}{\Delta}, \quad \Omega = \frac{A^2 \tan \delta^1 - A^1 \tan \delta^2}{\Delta}. \tag{34e-g}$$

Solving (34a,b) for $\dot{\gamma}$ and $\dot{\omega}$, obtain

$$\frac{1}{2}\dot{\gamma} = D_{11}^{p'} \frac{S_{11}}{S} + D_{12}^{p'} \frac{S_{12}}{S}, \quad \frac{1}{2}\dot{\omega} = D_{11}^{p'} \frac{S_{12}}{S} - D_{12}^{p'} \frac{S_{11}}{S}. \tag{35a,b}$$

Hence, $S\dot{\gamma}$ is the rate of the distortional plastic work associated with the stress-difference, \mathbf{S} , measured per unit reference volume.

The plastic deformation rates (34a,b) can be expressed in the following coordinate-independent form:

$$\mathbf{D}^{p'} = \dot{\gamma} \frac{\boldsymbol{\mu}}{\sqrt{2}} + \dot{\omega} \frac{\tilde{\boldsymbol{\mu}}}{\sqrt{2}}, \tag{36a}$$

where the unit tensor $\tilde{\boldsymbol{\mu}}$, orthogonal to $\boldsymbol{\mu}$, is defined by

$$\tilde{\mu}_{ij} = e_{ik} \mu_{kj}, \quad \tilde{\boldsymbol{\mu}} : \tilde{\boldsymbol{\mu}} = 1, \quad \boldsymbol{\mu} : \tilde{\boldsymbol{\mu}} = 0, \tag{36b-d}$$

and where e_{ij} is the two-dimensional permutation symbol, i.e., $e_{12} = -e_{21} = 1$, $e_{11} = e_{22} = 0$. The tensor $\tilde{\boldsymbol{\mu}}$ is proportional to the tensor $\hat{\boldsymbol{\mu}}$ of Balendran and Nemat-Nasser (1993a); see also Rudnicki and Rice (1975).

It is convenient to express $\tilde{\boldsymbol{\mu}}$ directly in terms of the deviatoric part of the total deformation rate tensor \mathbf{D}' as follows:

$$\tilde{\boldsymbol{\mu}} = a(\mathbf{1}^{(4s)} - \boldsymbol{\mu} \otimes \boldsymbol{\mu}) : \mathbf{D}', \quad a = \{|\mathbf{D}'|^2 - (\boldsymbol{\mu} : \mathbf{D}')^2\}^{-1/2}, \tag{36e,f}$$

where $\mathbf{1}^{(4s)}$ is the fourth-order symmetric identity tensor; see Nemat-Nasser and Hori (1993). Note that, in this representation, $\tilde{\boldsymbol{\mu}} = \mathbf{0}$ when \mathbf{D}' and $\boldsymbol{\mu}$ are coaxial. From (34) and (36), now obtain

$$\mathbf{D}^p = \dot{\gamma} \left\{ \frac{\boldsymbol{\mu}}{\sqrt{2}} + \frac{1}{2} \Gamma \mathbf{1} \right\} + \dot{\omega} \left\{ \frac{\tilde{\boldsymbol{\mu}}}{\sqrt{2}} + \frac{1}{2} \Omega \mathbf{1} \right\}, \tag{37}$$

and the effective plastic deformation rate, $\dot{\gamma}_{\text{eff}}$, becomes

$$\dot{\gamma}_{\text{eff}} = (2\mathbf{D}^{p'} : \mathbf{D}^{p'})^{1/2} = (\dot{\gamma}^2 + \dot{\omega}^2)^{1/2}, \quad \dot{\gamma} = \sqrt{2} \boldsymbol{\mu} : \mathbf{D}^p, \quad \dot{\omega} = \sqrt{2} \tilde{\boldsymbol{\mu}} : \mathbf{D}^p. \tag{38a-d}$$

The final constitutive equation is therefore given by

$$\dot{\boldsymbol{\tau}} = \mathcal{L} : (\mathbf{D} - \mathbf{D}^p) - \mathbf{W}^p \boldsymbol{\tau} + \boldsymbol{\tau} \mathbf{W}^p, \tag{39}$$

where \mathcal{L} is defined by (26h,i), and \mathbf{D}^p and \mathbf{W}^p by (37) and (34d), respectively.

For the special case when $\delta^1 = \delta^2 = \delta$, the results reported by Balendran and

Nemat-Nasser (1993a) are recovered. From (29c) it follows that, in such a case, at a minimum it must be required that $\boldsymbol{\beta}$ and \mathbf{S} be coaxial, as shown in Fig. 5. Then, $\sin 2\nu_0 = \cos \phi_\mu$, and it follows that

$$B^1 = B^2 \equiv B = \frac{\sin(\phi_\mu - \delta)}{\cos \delta}, \quad A^1 = A^2 \equiv A = \frac{\cos(\phi_\mu - \delta)}{\cos \delta}, \tag{40a-d}$$

$$\Delta = 2AB,$$

leading to

$$\dot{\omega} = B(\dot{\gamma}^1 - \dot{\gamma}^2) = 2B W_{12}^p, \quad \dot{\gamma} = A(\dot{\gamma}^1 + \dot{\gamma}^2),$$

$$\Omega = 0, \quad \Gamma = \tan \delta / A, \quad D_{kk}^p = \dot{\gamma}\Gamma. \tag{41a-f}$$

Eq. (37) gives the plastic deformation rate for a general continuum model of deformation of frictional granules, based on the double-sliding concept. It includes various other models as special cases. For example, when the fabric effects are neglected, $\boldsymbol{\beta} = \mathbf{0}$, and there are no plastically-induced volumetric strains, the model of Spencer (1964) is recovered. With $\boldsymbol{\beta} = \mathbf{0}$ and $\delta^1 = \delta^2$, the model of Mehrabadi and Cowin (1978) is obtained. When only $\delta^1 = \delta^2$, the model of Balendran and Nemat-Nasser (1993a) results. Note that $\delta^1 = \delta^2$ only when the fabric tensor is coaxial with the stress-difference tensor \mathbf{S} , as shown if Fig. 5.

8.1. Continuum approximation

In continuum plasticity, the terms associated with the plastically-induced spin, \mathbf{W}^p in (39), are generally neglected in defining the elasticity relations. Using this and a similar approximation for the evolution of the fabric tensor in (21c), consider the elasticity and fabric-evolution relations given by

$$\dot{\boldsymbol{\tau}} \approx \mathcal{L}:(\mathbf{D} - \mathbf{D}^p), \quad \dot{\boldsymbol{\beta}} \approx A\mathbf{D}^{p'} + \frac{\dot{p}}{p}\boldsymbol{\beta}, \tag{42a,b}$$

where the elasticity tensor \mathcal{L} is still defined by (26h,i), but the plastically-induced deformation rate is now *approximated* by

$$\mathbf{D}^p = \dot{\gamma} \frac{\boldsymbol{\mu}}{\sqrt{2}} + \alpha(\mathbf{1}^{(4s)} - \boldsymbol{\mu} \otimes \boldsymbol{\mu}):\mathbf{D}' + \frac{1}{2}\dot{\gamma}\Gamma\mathbf{1}, \tag{43}$$

where $\alpha = \frac{\dot{\omega}a}{\sqrt{2}}$ is the noncoaxiality factor.

From the yield condition (11b), consider the consistency relation

$$\dot{S} - \dot{p}M = p\dot{M}, \quad M = \sin \phi_\mu. \tag{44a,b}$$

Since pM defines the size of the yield circle, its rate of change gives the workhardening parameter. In general, M is a function of the void ratio and other

parameters which characterize the microstructure of the granular mass. As an illustration, let

$$M = M(\gamma, \Delta), \quad \gamma = \int_0^t \sqrt{2} \boldsymbol{\mu} : \mathbf{D}^p dt, \quad \Delta = \int_0^t \frac{\rho_0}{\rho} D_{kk}^p dt, \quad (45a-c)$$

where γ is some measure of the accumulated plastic strain, and Δ is the total accumulated plastic volumetric strain, measured relative to a reference state with mass density ρ_0 , the current mass density being ρ ; see Nemat-Nasser and Shokoh (1980). Then, it follows that

$$\dot{M} = H\dot{\gamma}, \quad H = \frac{\partial M}{\partial \gamma} + \frac{\partial M}{\partial \Delta} \frac{\partial \Delta}{\partial \gamma}. \quad (45d,e)$$

Hence, H is the workhardening parameter.

The left-hand side of (44a) can be computed explicitly, using (42a,b), (43), and (23). One obtains

$$\begin{aligned} \dot{S} - \dot{p}M &= G(\sqrt{2}D_\mu - \dot{\gamma}) + \bar{G}\mu_\beta \left\{ \sqrt{2}(1 - \alpha)D_\beta + \mu_\beta(\sqrt{2}\alpha D_\mu - \dot{\gamma}) \right\} \\ &\quad - \frac{1}{2}\dot{\gamma}A + \bar{K}\mu_\beta(D_{kk} - \dot{\gamma}\Gamma) + K(D_{kk} - \dot{\gamma}\Gamma)(\beta\mu_\beta/p + M). \end{aligned} \quad (46a)$$

where $D_\mu = \mathbf{D} : \boldsymbol{\mu}$, $\mu_\beta = \boldsymbol{\mu}_\beta : \boldsymbol{\mu}$, $D_\beta = \mathbf{D} : \boldsymbol{\mu}_\beta$, and β is given by (8a). These quantities are all in terms of the current stress and fabric state and the deformation rate tensor. Substitution from (46a) and (45d) into (44a) yields an expression for $\dot{\gamma}$, as follows:

$$\dot{\gamma} = \frac{\sqrt{2}GD_\mu + \sqrt{2}\bar{G}\mu_\beta[(1 - \alpha)D_\beta + \alpha D_\mu\mu_\beta] + \bar{K}D_{kk}\mu_\beta + KD_{kk}(\beta\mu_\beta/p + M)}{pH + G + \bar{G}\mu_\beta^2 + \bar{K}\Gamma\mu_\beta + \frac{1}{2}A + K\Gamma(\beta\mu_\beta/p + M)}. \quad (46b)$$

To obtain an expression for the dilatancy parameter Γ , consider the rate of stress work, $\boldsymbol{\tau} : \mathbf{D}^p$, and equate this to the rate of dissipation, $pM_f\dot{\gamma}$, to obtain

$$\Gamma \approx -M_f + M + \frac{\beta}{p}\mu_\beta, \quad 0 < M = \sin \phi_\mu \leq 1, \quad (47a,b)$$

where (11b) is used, and the term proportional to $D_\beta - D_\mu\mu_\beta$ is neglected. Since $\boldsymbol{\mu}$ and $\boldsymbol{\mu}_\beta$ are unit deviatoric tensors, $\mu_\beta = \cos 2\theta$, where θ is the angle between the major principal directions of the stress-difference, \mathbf{S} , and the fabric, $\boldsymbol{\beta}$, tensors. Hence, $-1 \leq \mu_\beta \leq 1$. The maximum fabric-induced dilatancy occurs for $\theta = 0$, i.e., when S_1 and β_1 are coincident, while there is a maximum densification due to the fabric when these directions are 90 degrees out of phase. The latter often occurs in unloading.

In addition to the elasticity moduli, C_{ij} , which must be evaluated

experimentally, or calculated based on some micromechanical model, there are four material functions in this continuum model. These are:

1. The noncoaxiality parameter, α , which, from (33b) and (41a), depends on the friction and dilatancy parameters, M and Γ in the continuum case;
2. The friction coefficients M and M_f , which are both dependent on the void ratio (defined as the ratio of the void volume divided by the solid volume, $e = V_v/V_s$), or the volumetric strain, $\Delta = (e_0 - e)/(1 + e_0)$, and possibly on the strain measure γ , where e_0 is the reference void ratio. As a general guide, consider $M = f_1(e_M - e, e - e_m)$, where e_M and e_m are the maximum and minimum void ratios, reflecting also the grain size and its distribution. A similar representation can be used for M_f .
3. The parameter A in (42b), which defines the evolution of the fabric tensor β . It may be assumed that A is a function of $(1 - \mu_\beta/\mu_s)$, where μ_s is the saturation value of μ_β .
4. The above-mentioned constitutive parameters must be restricted such that the void ratio, e , remains non-negative and less than the maximum value, e_M . Generally, it must be required that $0 < e_m \leq e \leq e_M$, where both e_m and e_M depend on the grain characteristics (sizes, shapes, their distribution), and the pressure.

It is not too difficult to extend this model to the three-dimensional case, as well as to a rate-dependent one.

Acknowledgements

The work reported here has been supported in part by the Army Research Office under Contract DAAHO4-96-1-0376, and in part by the National Science Foundation under Grant CMS-9729053, with the University of California, San Diego.

References

- Balendran, B., Nemat-Nasser, S., 1993a. Double sliding model cyclic deformation of granular materials, including dilatancy effects. *J. Mech. Phys. Solids* 41 (3), 573–612.
- Balendran, B., Nemat-Nasser, S., 1993b. Viscoplastic flow of planar granular materials. *Mech. Mat.* 16, 1–12.
- Christoffersen, J., Mehrabadi, M.M., Nemat-Nasser, S., 1981. A micromechanical description of granular material behavior. *J. Appl. Mech.* 48, 339–344.
- de Josselin de Jong, G. (1959), Statics and kinematics in the failable zone of granular material, Thesis, University of Delft.
- Hill, R., 1950. *Mathematical theory of plasticity*. Oxford University Press, Oxford.
- Mandel, J., 1947. Sur les lignes de glissement et le calcul des déplacements dans la déformation plastique. *Comptes rendus de l'Académie des Sciences* 225, 1272–1273.
- Mehrabadi, M.M., Cowin, S.C., 1978. Initial planar deformation of dilatant granular materials. *J. Mech. Phys. Solids* 26, 269–284.

- Mehrabadi, M.M., Loret, B., Nemat-Nasser, S., 1993. Incremental constitutive relations for granular materials based on micromechanics. *Proc. Roy. Soc. Lond. A* 441, 433–463.
- Mehrabadi, M.M., Nemat-Nasser, S., Oda, M., 1982. On Statistical description of stress and fabric in granular materials. *Int. J. Num. Anal. Methods in Geomechanics* 6, 95–108.
- Mehrabadi, M.M., Nemat-Nasser, S., Shodja, H.M., Subhash, G. 1988. Some basic theoretical and experimental results on micromechanics of granular flow, in *Micromechanics of granular materials*. In: Satake, M., Jenkins, J.T. (Eds.), *Proc. 2nd US-Japan Sem. Mech. Granular Mat., Sendai-Zao, Japan*. Elsevier, Amsterdam, pp. 253–262.
- Nemat-Nasser, S., 1980. On behavior of granular materials in simple shear. *Soils and Foundations* 20, 59–73.
- Nemat-Nasser, S., Hori, M., 1999. *Micromechanics: overall properties of heterogeneous solids*, 2nd revised edition. Elsevier, Amsterdam.
- Nemat-Nasser, S., Mehrabadi, M.M., Iwakuma, T. 1981. On certain macroscopic and microscopic aspects of plastic flow of ductile materials. In: Nemat-Nasser, S. (Ed.), *Three-dimensional constitutive relations and ductile fracture*. North-Holland, Amsterdam, pp. 157–172.
- Nemat-Nasser, S., Shokooh, A., 1980. On finite plastic flow of compressible materials with internal friction. *Int. J. Solids Struct.* 16 (6), 495–514.
- Oda, M., Konishi, J., Nemat-Nasser, S., 1982. Experimental micromechanical evaluation of strength of granular materials: effects of particle rolling. *Mech. Mat.* 1 (4), 269–283.
- Okada, N., Nemat-Nasser, S., 1994. Energy dissipation in inelastic flow of saturated cohesionless granular media. *Geotechnique* 44 (1), 1–19.
- Rudnicki, J.W., Rice, J.R., 1975. Conditions for the localization of deformation in pressure-sensitive dilatant materials. *J. Mech. Phys. Solids* 23, 371–394.
- Spencer, A.J.M., 1964. A theory of the kinematics of ideal soils under plane strain conditions. *J. Mech. Phys. Solids* 12, 337–351.
- Spencer, A.J.M. 1982. Deformation of ideal granular materials. In: Hopkins, H.G., Sewell, M.J. (Eds.), *Mechanics of solids*. Pergamon, Oxford, pp. 607–652.
- Subhash, G., Nemat-Nasser, S., Mehrabadi, M.M., Shodja, H.M., 1991. Experimental investigation of fabric-stress relations in granular materials. *Mech. Mat.* 11 (2), 87–106.